

Fabricable Dihedral Escher Tessellations

Submission ID: 35

Abstract

The growing popularity of 3D digital manufacturing has spurred a high demand for accessible methods for designing and fabricating customized 3D objects. In this paper, we present a novel approach to model and fabricate Escher dual-shape tilings from user-defined shapes. In a nutshell, Escher's dual shape tiling method smoothly transforms one tile pattern into another, generating a dual perception effect of the two shapes. We adapt Escher's dual shape tiling and perception effect to 3D manufacturing. Thus, our method takes two user-defined shapes and computes their dual shape tiling. A key feature of our method is that the dual shape patterns utilize solid and hollow space simultaneously. Specifically, our technique maps one shape to solid structure, while the second shape is mapped to hollow background, optimizing both spaces and bringing higher utilization of materials. To conform with 3D printability requirements, our tiling computation accounts for connectivity and strength as well as dense packing for efficiency. Our dual shape tiling algorithm gives rise to novel manufacturing applications such as ornamental texturing with dual perception Escher patterns, decorative window blinds, flexible tiling patterns, and shade effects.

Keywords: Shape modeling, Dihedral tessellation, Digital fabrication.

1. Introduction

3D manufacturing is rapidly progressing towards mass usage, with goals to enable non-professionals to easily manipulate and customize their 3D models into creative and beautiful products. Therefore, in recent years there has been significant research dedicated to providing computational tools for a wide range of shape manipulation and customization tasks for 3D printing. Among others, researchers have introduced novel techniques and applications such as balancing the manufactured shapes [1], creating spinnable objects [2], turning surfaces into physical filigrees [3], stenciling decorative patterns [4], designing shapes as musical wind instruments [5], lampshades with projecting light control [6], models generating playful shadows [7], embedding QR codes [8] and helping users maintain printability during modifications [9].

In this paper, we study the modeling and fabrication of customized decorative patterns obtained by computing tilings of two shapes that coexist together. Dual shape tilings are mostly well-known from Escher's works, as a form of graphical art offering a dual perception mechanism. Specifically, the foreground-background assignment of neighboring shapes can reverse depending on the viewer's focal attention. Escher intentionally employed dual figure-ground arrangements to reveal the ambiguities of visual perception and categorization. Their simplicity yet exciting perceptual effects, turned Escher's dual tiles into ubiquitous art and design structures [10].

In our work, we adapt Escher's dual tiles for artistic and decorative 3D printing purposes. Thus, we demonstrate their application to 3D manufacturing of decorative textured shapes. Our 3D tiles can be joined by hinges and connectors to form articulated Escher tilings. We utilize this dynamic pattern and apply it to create window blinds and dynamic structures that can be fabricated using a home printer. To the best of our knowledge, this is the first attempt to apply Escher's dual tiles to 3D manufacturing.

Decorative and artistic tools have been previously introduced in the context of 3D manufacturing. In general, these works, manipulate the printable 3D shape in search for novel applications to enrich 3D manufacturing. Nevertheless, the majority

of these methods design artistic effects by focusing on the solid shape [11] or on the hollow space that emerges from the printed solid structure [6, 7]. Our work, however, utilizes both solid and hollow spaces simultaneously. The method computes a dual shape tiling where the first shape is defined by the solid printed parts while the second shape emerges from the contour of the complementary background. **The utilization of both solid and hollow spaces on the given surface introduces novel artistic and aesthetic effects as well as having the advantage of simplifying the overall structure and saving printing material.**

The dual shape tiling is computed by optimizing the solid shape together with its complementary background while preserving visual shape properties such as contour and geometric features for each of the two shapes. To account for 3D printability, solid tiles, as well as complementary hollow tiles, should adhere to strength requirements. In our case, solid tiles should be partially connected using connectors wider than the minimum printing accuracy, while hollow parts should remain unconnected. We denote this condition as *mutual surroundings constraint*. We observe that this problem can be reduced to a dihedral tessellation problem in the plane under the constraint of mutual encirclement.

2. Related Work

Our related work discussion is divided into surveying Escher tilings computation, manufacturing of tiling patterns and mosaics, and packing.

2.1. Escher tilings

A tiling of the plane is a collection of shapes that cover the plane without any gaps or overlaps. Dual tiling patterns a.k.a “figure-ground” patterns may be observed as early as the nineteenth century in drawings of Koloman Moser. Most famous is M.C. Escher work in the first half of the twentieth century, which studied the regular division of the plane into tiles. In particular, he produced a large collection of ingenious tessellations [10],

made from motifs resembling people, animals, and fantasy creatures. Following, Dress [12] has introduced a specific class of dihedral Escher tilings called “Heaven and Hell patterns” and Grünbaum and Shephard’s [13] have defined the mathematics behind tiling and geometric patterns.

“Escherization” was initially termed by Kaplan and Salesin [14] as a problem in computer graphics of tiling a plane with a given closed figure. The method modifies the given figure to conform to an isohedral tiling pattern. In a follow-up [15], authors extend their method to admit two shapes tilings using dihedral tiling patterns.

Yen and Séquin [16] developed a method to compute *Escher Spheres*, i.e., Escher tiles that are assembled on a sphere domain through a tiling deformation. Similar to us, Howison and Séquin [17] adapt Escher tiles for 3D manufacturing purposes. In their work, they investigate 2.5D isohedral tilings through extrusion and manual mesh editing. They also show 3D isohedral tilings using predefined lattices. In contrast, our technique is automatic and produces Escher dual-shape tilings that are 3D printable, allowing novel effects and applications.

Dual shape Escher tilings were explored [18] to generate a gradual transformation between the two shapes and obtain the dual perception effect. Escherization tiling has been formulated as a maximum eigenvalue problem to allow more intricate and complex tile shapes [19]. The shape optimization is also explored using interactive genetic algorithms [20] to find a shape for isohedral Escher tilings. In common to these works is finding a minimal modification for generating feasible single shape tiling patterns.

Recently Lin et al. [21] proposed a framework integrating matching and warping to generate Escher-like tiles transformations for dual shape perception. Our work has similar components addressing the dual shape tiling; however, ours is 3D fabrication oriented accounting for specific printability and application requirements.

2.2. Fabricable tilings

With the growing popularity of 3D digital manufacturing, researchers have paid much attention to the problem of generating geometric patterns to decorate surfaces with the purpose of customization and enhancement of 3D printing.

Ornaments were applied to fabricated 3D objects by synthesizing 1D patterns along curves with restricted topology [22]. Similarly, synthesized printable 3D patterns were demonstrated by modifying texture synthesis to conform with a base surface [23]. Martinez et al. [24] synthesized flat shapes for laser cutting manufacturing and Chen et al. [3] synthesized filigree-like structures along surfaces. Their approach synthesizes a set of base elements along a target surface by preserving their appearance and allowing overlaps.

Zehnder et al. [25] introduced a method for interactive design with curve networks as ornamental priors onto 3D surfaces. In their work, the user positions curve elements onto a surface, which are then deformed using elastic rods simulation. Schumacher et al. [4] introduced a method to allow artistic cutouts into shell objects by removing material while accounting for printability and stability. Chen et al. [11] further proposed a method for synthesizing flat tile patterns on a base surface, such that the planar tiles can be easily printed and assembled afterwards. Recently Schüller et al. [26] introduced a novel fabricable-friendly tiling called “zippable”. In their work, they represent a 3D model with a single, long ribbon with a zipper around its boundary. In this approach, some distortion may occur to areas on the model.

These works are concerned with mapping and printing 3D tilings onto arbitrary surfaces. Nevertheless, our technique involves 2D and 2.5D tilings in the plane, thus avoiding 3D mapping problems. Our method focuses on dual-shape tilings and the geometric relations between the solid and hollow parts in the manufactured patterns and their applications.

2.3. Mosaics tiles and packing

Mosaics are a form of art in which a large image is formed by placing together a collection of small images tiles. Photomosaics [27] are a collection of small images arranged in a rectangular grid in such a way that when they are viewed together from a distance, they suggest a larger image. Simulated Decorative Mosaic [28] approaches the problem of aligning square tiles with varying orientations to preserve input image edges while maximizing the area covered by the colored tiles.

Related to mosaics, tiling is the packing problem that has been extensively studied in computational geometry with application to a broad spectrum of layout problems, such as for cloth, leather, and glass. Since the packing problem is NP-hard [29], numerous heuristics have been developed. Kim and Pellacini [30] obtain a tighter mosaic packing by minimizing an energy function for a new kind of mosaics called Jigsaw Image Mosaic (JIM). To obtain the closest mosaic arrangement with no overlapping, Hu et al. [31] sample the surface according to the curvature and redivide it using the chordal axis transform (CAT) obtaining optimal positions for the tiles elements. Kwan et al. [32] proposed a novel shape descriptor for computing the filling collage pattern. The major difference with our problem is that no adjacency constraints are considered in the above methods.

3. Overview

Given two user-defined shapes S_1, S_2 , our algorithm computes an optimized dihedral tiling following four tiling rules while optimizing the shapes to account for tiling adjacency, printability requirements, and preserve their visual appearance.

Since the compatibility between S_1 and S_2 has a significant impact on the quality of the final result T_1, T_2 , it is more convenient for non-professional users to manually specify S_1 and let the system suggest a set of best candidates for S_2 from a database. Both options are offered by our design framework and they share the same methodology.

Starting with one of the shape S_1 , we compute a quadrilateral polygon from its sample points. To compute a tiling of the plane from the initial quadrilateral, we define four tiling rules that satisfy the mutual surroundings constraints.

Next, we use the enclosed space M between the four tile shapes of S_1 to define the complementary (hollow) dual shape pattern and match S_2 to it. Then we morph this tiling configuration into the transformed shapes T_1, T_2 such that they couple together and conform to printability requirements while preserving the visual appearance of the original shapes S_1, S_2 as much as possible.

Our algorithm exhaustively searches for the best tiling pattern while simultaneously optimizing the two shapes to minimize their distortion and achieve an optimal tiling. The dual shape tiling can be applied as texture on a 3D surface to follow a 3D printing process. The algorithm pipeline is illustrated in Figure 1.

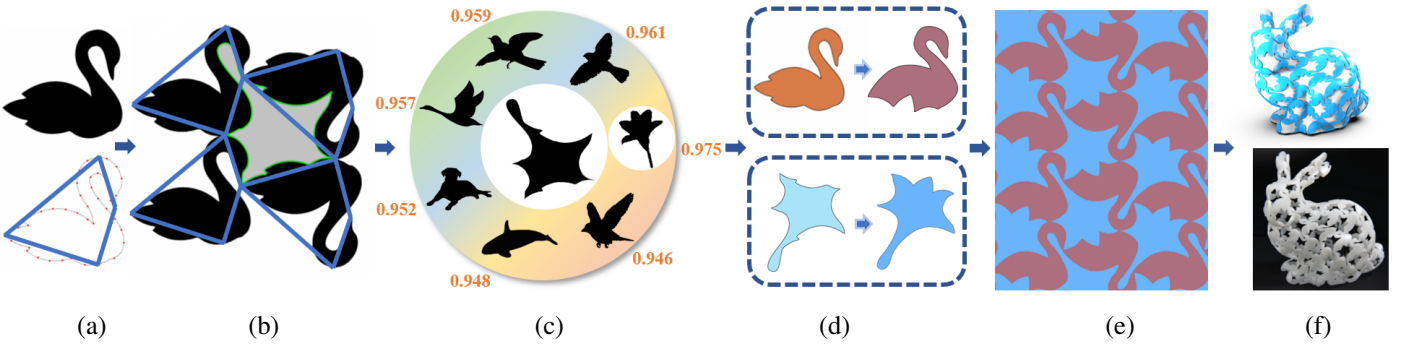


Figure 1: Given a target shape and its quadrilateral polygon (a), we compute a rule-based four tiles pattern (b) and find the best matching shape to the enclosed tile from a database (c). We simultaneously morph the two shapes (d) such that they couple together, while preserving their visual appearance (d), resulting in a fabricable dual Escher tessellation (e) that can be mapped on a 3D object and efficiently manufactured (f).

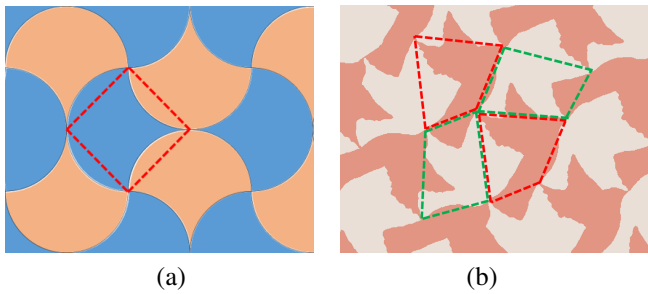


Figure 2: Escher’s artworks using Isohedral (a) and dihedral (b) tilings. Tiling polygons are marked by dash lines.

4. Technical Details

4.1. Dihedral Tiling Generation

A tiling of the plane is a collection of tiles that cover the plane without any gaps or overlaps. A tiling vertex is a point where three or more tiles meet. A tiling is dihedral if the tiling consists of two different tile shapes that are adjacent in the tiling (Figure 2). We refer to [15] for further detailed definitions of dihedral tilings.

Our technique generates a two shape tiling where the first shape is contained in the foreground solid tile while the second shape is contained in the background similar to [21].

Starting with one of the shapes, we compute its corresponding quadrilateral tiling polygon by randomly selecting four points from the candidate points composed of feature points according to local curvature and uniformly sampling points between feature points. Next, we define four tiling rules for placing the initial quadrilateral tiling polygon and generate a dihedral tiling pattern (see Figure 3). Following these rules, the tiling pattern can be extended to the whole plane through repeated replications of the initial tile.

Essentially, these rules define a replication schemes of the initial tiling polygon into a grid-like four tile arrangement. The rules guarantee that the four tiles are touching each other, enclosing an isolated surface in their interior, which defines the dual background tile.

Translation rule. Translate P_1 (P_i is the i-th tile) along the diagonal vector $\vec{13}$ (\vec{pq} is the vector from vertex #p to #q) to obtain P_2 . Translate P_1 and P_2 along the diagonal vector $\vec{24}$ to obtain P_3 and P_4 respectively. (Figure 3a).

Flipping rule I. Translate P_1 along the diagonal vector $\vec{24}$ to obtain P_3 . Flip P_1 and P_3 , and translate along the diagonal vector $\vec{13}$ to obtain P_2 and P_4 respectively. (Figure 3b).

Flipping rule II. Translate P_1 along the diagonal vector $\vec{13}$ to obtain P_3 . Flip P_1 and P_3 , and translate along the diagonal vector $\vec{24}$ to obtain P_2 and P_4 respectively. (Figure 3c).

Rotation rule. Rotate P_1 around its tiling vertex #1 180 to obtain P_2 . Rotate P_2 around its tiling vertex #2 180 to obtain P_3 . Rotate P_3 around its tiling vertex #3 180 to obtain P_4 . This rule has is applicable only for parallelograms, otherwise the four elements cannot enclose a dual tile in their interior. (Figure 3d)

The above rules are a subset selection from the twelve “heaven and hell” tiling rules in [15]. Specifically, the translation rule corresponds to (IH01;1,4), flipping rules correspond to (IH03;2,5) and rotation rule corresponds to (IH47;2 $\frac{1}{2}$,4 $\frac{1}{2}$). Our motivation behind this selection of rules is that they generate nicely shaped quad tiles. Thus, they allow fitting shapes in their interior with minimal distortion.

Note that collisions between shapes may still occur when fitted to the quad tiles. In such cases, we avoid the specific tiling rule and keep only the valid tiling schemes.

4.2. Shape Matching and Morphing

With the above tiling rules, we search for the best matching tiling scheme followed by morphing the shapes to fit these tiles. Given a polygonal shape S_1 , we uniformly sample its contour and compute its features at high curvature points. This yields a set of candidate tiling vertices.

We perform an exhaustive search, selecting each time four ordered points from the candidate set as a tiling polygon, generating quadrilateral tiling patterns according to our rules and computing a shape matching energy function. Our technique commences once a sufficient tiling has been found in terms of shape matching quality as measured by the energy function.

Shape matching. Matching S_1 to a tile is straightforward as foreground quadrilaterals tiles are created by sampling four points in S_1 . Therefore S_1 and its tile simply match at those four points.

We denote the enclosed space between the four tiled shapes (S_1) by M . The contour of M is extracted by connecting the tiling vertices in the pattern. For each tiling rule, we have a different order to preserve a consistent counterclockwise contour order (see Figure 3).

Given the contour of M , we compute a best matching of S_2 to M . If a database is given, our method retrieves a subset of top

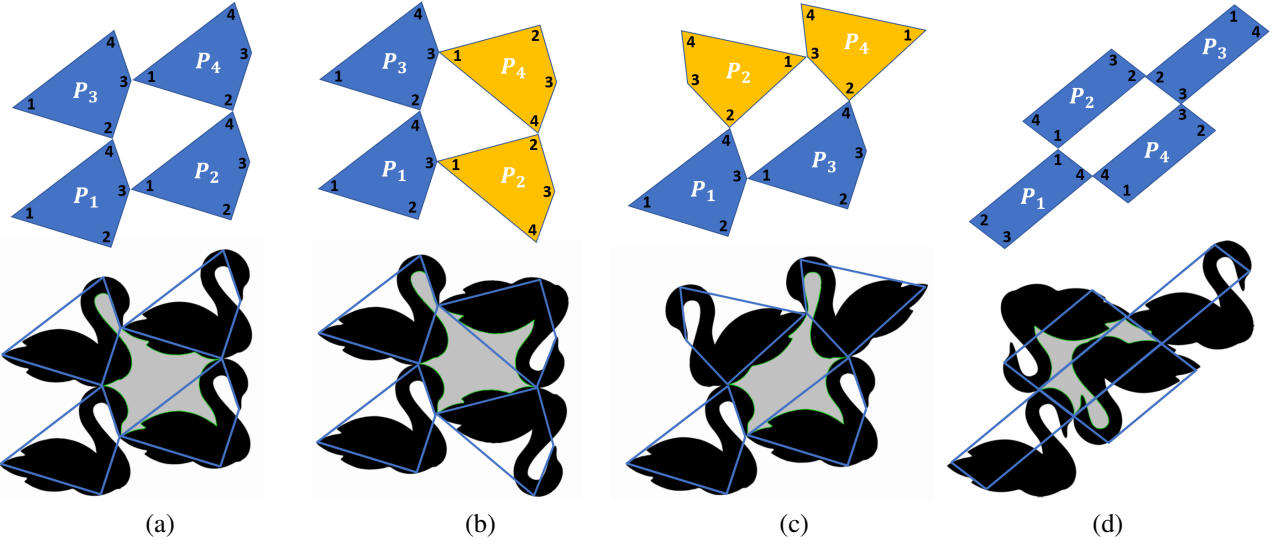


Figure 3: Dihedral tiling rules: translation rule (a), flipping rule I (b), flipping rule II (c) and rotation rule (d). Upper row shows tiling polygons (flipped ones are in yellow) and lower row is the resulting tiling of the swan shape.

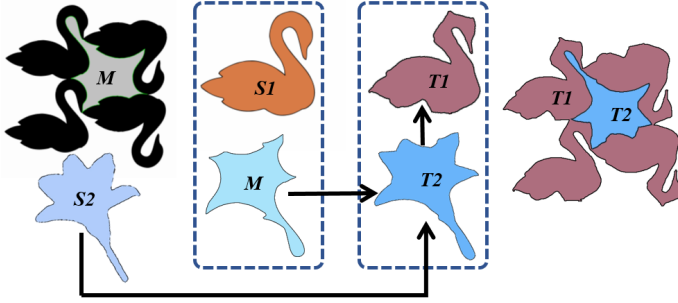


Figure 4: Morphing. Starting from S_1 and M , the optimized shapes T_1 and T_2 are obtained by morphing between M and S_2 .

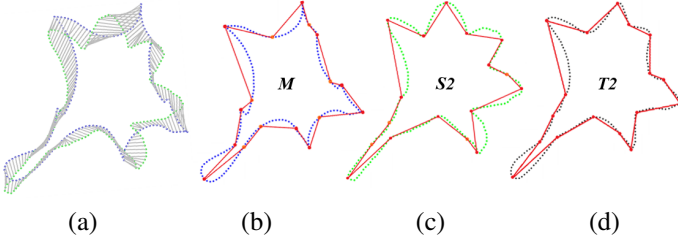


Figure 5: Alignment of M and S_2 based on shape correspondence (a); Frame polygons of M and S_2 [33] (b, c, in red); Morphing result T_2 (d).

candidates according to their matching energy to M , and the user selects the most adequate shape as S_2 .

To calculate the matching between two contours, we use the triangle-area representation (TAR) and measure with it the similarity between matching points on the shapes contours [34]. This representation is effective in capturing both local and global characteristics of a shape, invariant to translation, rotation, and scaling, and robust against noise and moderate amounts of articulation. In the matching stage, we employ a dynamic space warping (DSW) algorithm to search efficiently for the optimal (least cost) correspondence between the points of two shapes.

To accelerate the whole shape retrieval process, we introduce a fast-reject filtering stage to avoid the costly similarity computation for too distinct shapes in the database. We use a 2D shape

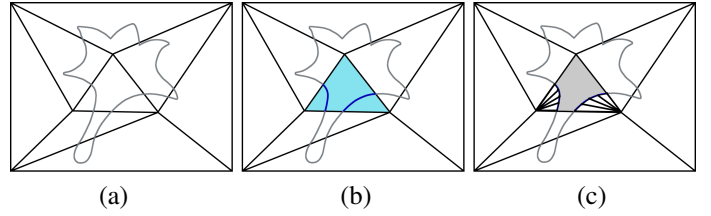


Figure 6: Mesh difference. Input pattern contour overlayed on the mesh (a). Boolean difference between a triangle and the input contour (b) and the resulting constrained Delaunay triangulation remeshing the intersection region (c).

compactness - isoperimetric quotient signature, as our fast reject filter. It is defined as the ratio between the shape area and that of the circle having the same perimeter.

Shape morphing. Starting from the initial tiling configuration defined by the four tiles of S_1 and the enclosed shape M , our aim is to find an optimal transformation of S_1 and M into transformed shapes T_1 and T_2 with the objectives that they are as close as possible to S_1 and S_2 thus preserving their visual appearance (see Figure 4).

We formulate the objective function to measure the visual quality of the transformed shapes T_1 and T_2 as follows:

$$E_{sim}(T_1, T_2) = \lambda F(T_1, S_1) + (1 - \lambda) F(T_2, S_2) \quad (1)$$

where λ allows weighing each shape deformation independently. In our experiments $\lambda = 0.5$, however if required could give higher priority to S_1 over S_2 thus increasing λ . F measures the degree of deformation from S to T and is defined as:

$$F(T, S) = \varphi(T, S) + Insec(T, S) - \omega'(T, S) \quad (2)$$

where $\omega(T, S)$ is a shape similarity function based on TAR descriptors [34]. $\varphi(T, S)$ is the area function defined as:

$$\varphi(T, S) = (Area(T \cup S) - Area(T \cap S))/Area(T \cup S)), \quad (3)$$

$Insec(T, S)$ is a score that penalizes self-intersections in T or S with a high score in the range $[1 - 2]$.

To minimize $E_{sim}(\lambda, T_1, T_2)$ and maintain the coupling of T_1 and T_2 , we perform shape morphing between M and S_2 . The

shape T_1 is defined from the distortion of T_2 (specifically the tiling points) and the overall quadrilateral tiling pattern.

We employ the method of [33] to compute shape morphing, which is a two-level hierarchical interpolation algorithm. First, M and S_2 should be aligned together based on the correspondence obtained from the shape matching stage (Figure 5a). We compute the frame polygons of M and S_2 from the tiling vertices and feature points. Thus, we iteratively morph into intermediate shapes, to obtain the optimized result of T_1 and T_2 (Figure 5b-c).

Note that the four tiling vertices stay fixed through the morphing process thus ensuring the connectivity of tiles in the final tiling. This is essential for printability requirements in the 3D manufacturing process.

4.3. 3D Printable Tilings

In the final step, we transfer our 2D dual tiling into a structurally sound 3D texture structure. For given a 3D model, we first compute its parametrization onto a 2D plane. Then, we compute a boolean difference between our tiling pattern and the two-dimensional triangular mesh. We generate the hollow parts corresponding the secondary shape in the tiling and reconstruct the surface. Finally we perform structural optimization to conform to printability requirements and obtain the target model.

Mesh parametrization and boolean difference. To map the input 3D mesh model onto a 2D parameter domain, we use the as-rigid-as-possible parametrization approach [35] since it preserves proportions of the tessellation structure and minimizes distortions.

We then overlay the 2D tiling pattern onto the parameterized mesh and compute the cutout difference between the surface mesh and the tiling pattern contour. We remove these cutouts and remesh the remaining surface mesh utilizing a constrained Delaunay triangulation (Figure 6).

In the original tiling scheme, tilings connect to each other by tiling vertices that are not structurally stable for printability. We enhance stability by dilating contours, thus thickening the connectors between these contours. The conversion from points to connectors transform the hollow pattern into isolated components, which can be easily subtracted using the boolean difference to obtain a planar tiling of the triangular mesh.

Note that during the parametrization of closed shapes, they are cut into planar disk topologies yielding seams in the tiling pattern along these cuts. The parametrization of high genus models requires multiple cuts. Our parametrization technique aims at positioning these cuts in non-salient regions like the back or bottom of the model.

3D printability and structural enhancement. We map back the planar triangular mesh to three-dimensional space to obtain a 3D dual-tile shell model \mathcal{M} (i.e., a thick surface in 3D). Thus, \mathcal{M} is extruded by extruding each vertex along its normal direction (both positive and negative) by a default offset defining the shell thickness (in highly curved areas, self-intersections may occur when extruding the 3D shell model). The initial solid model \mathcal{M}_S is generated using Poisson surface reconstruction [36]. In all our experiments, the initial thickness is set to 1.2mm to satisfy printing constraints.

To enhance the stability of the physical model, structural optimization is performed. First, we perform structural analysis via finite element methods (FEM) on \mathcal{M}_S and obtain the von Mises stress for each element. To simulate stress, we fix the bottom part of the model and apply uniform pressure on the model. We use tetrahedral element here and employ the commercial software ABAQUS for stress analysis.

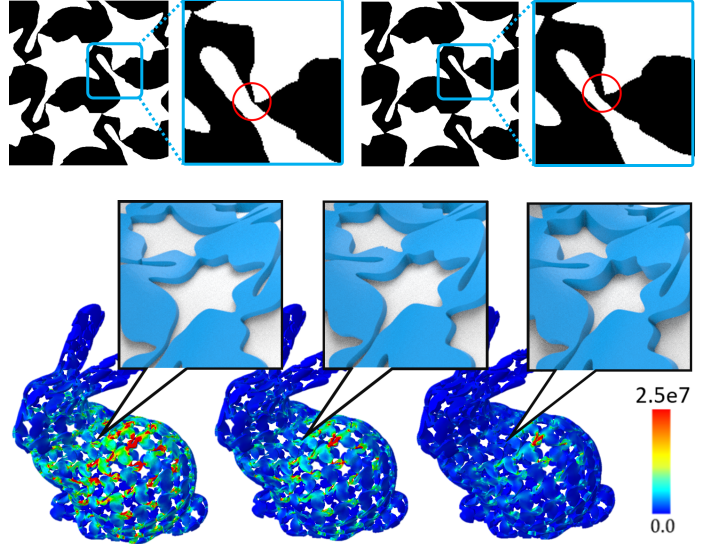


Figure 7: Structural optimization. Top row, tiling vertices are enlarged in width for structural soundness. Bottom row shows iterations of local thickness optimization and the resulting stress distributions on the bunny model.

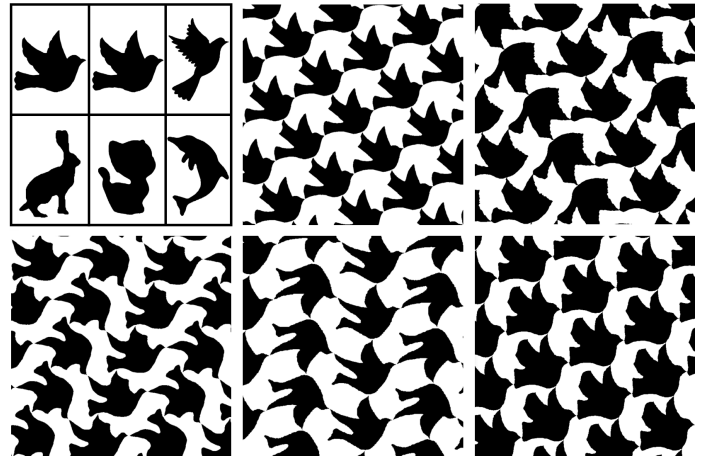


Figure 8: Given a dove shape (top left) as input, our system generates the top five dihedral tiling results. The matched shapes from the dataset are also listed in the top. The first result (top middle) takes the same shape as the dual.

By default, we consider forces that are applied from all directions; however, specific strength requirements like pressing and holding may be easily incorporated in our optimization. E.g., in the bunny model in Figure 7, we fix the bottom of the bunny and perform a 1000N downward force on its back.

We perform a two-step optimization scheme to increase strength. First, we enforce connectivity between the weak part and its solid neighborhood through increasing the area of connectors. Next, we increase the thickness of the model for each weak surface vertex. We iteratively solve the optimization problem with the following objective function:

$$\operatorname{argmin} \mathcal{V}(\mathcal{M}_S(R(\mathbf{x}), D(\mathbf{v}))) \text{ s.t. } SF(\mathcal{M}_S, \mathcal{F}) < \chi \quad (4)$$

where $\mathcal{V}(\cdot)$ is the total volume of the foreground solid space, $R(\mathbf{x})$ is the solid neighborhood of each tiling vertex \mathbf{x} , $D(\mathbf{v})$ indicates the thickness for each vertex \mathbf{v} on the mesh surface, $SF(\mathcal{M}_S, \mathcal{F})$ is the stress field computed from foreground solid model \mathcal{M}_S under the external forces \mathcal{F} , and χ is the yielding value for the material ($\chi = 20MPa$ for PLA in our experiments).

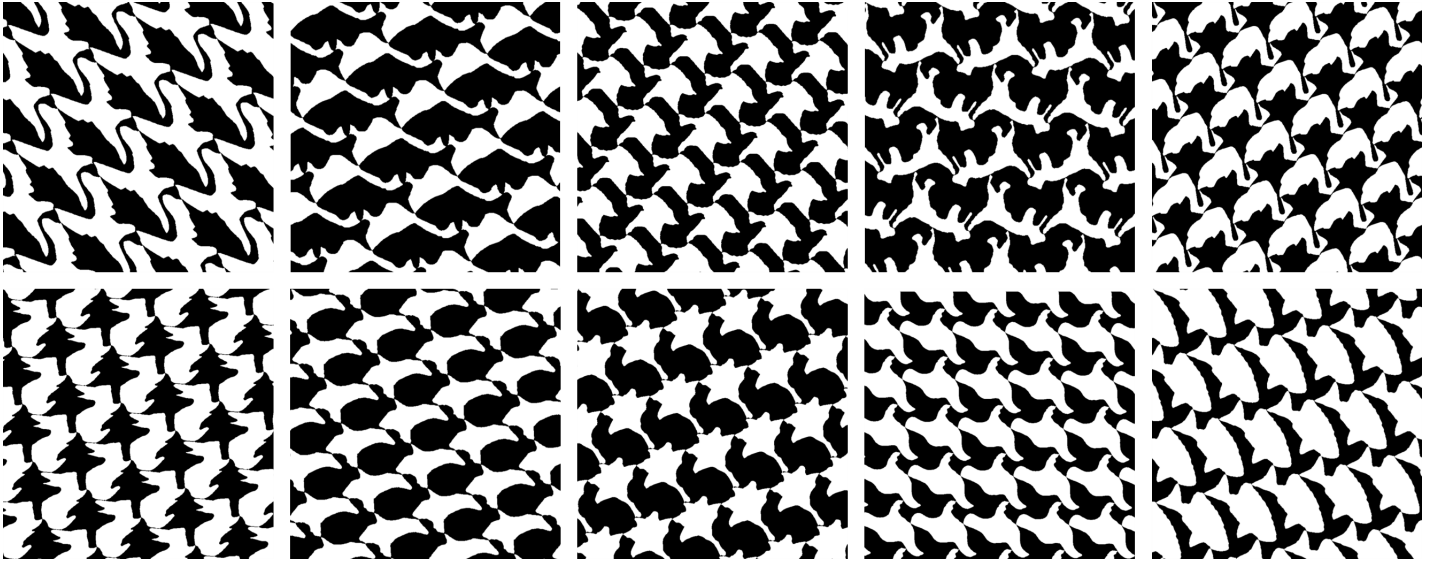


Figure 9: Various dual-shape tiling patterns generated by our system.

During the optimization, we first **locally dilate the contour of the primary (solid) shapes in the weak areas** to increase the connection area of the tiling vertices by a step size, until reaching the upper bound. The upper bound in connection area enlargement is 1% of the 3D shape's diagonal length. Then we increase the local thickness for the weak regions. We iteratively perform the two structural optimization steps, as shown in Figure 7.

5. Results and Discussions

We implemented our method and tested it on an Intel® Core™ i7-7700K CPU @ 3.6GHz and 16GB RAM. We have also created a database of shapes to allow the user to retrieve and select the best matching dual shapes for a user-defined primary shape. Our dataset is based on the MPEG-7 dataset [37], which we have enriched with additional images from the Internet. The dataset consists of 500 shapes, each represented by its polygonal contour.

Performance. Given one shape, our system suggests dual shapes for which the tiling best preserves visual appearance such that the users can select for further design (Figure 8). This works better than asking the user to predefine two input shapes as it might need high artistic background.

Given a pair of shapes, it takes approximately 20 seconds to generate a tiling pattern. If a choice of best matching dual shapes is requested, shape retrieval for best matching candidates is a time-consuming query and scales linearly with the database size. In our experiments, querying our database of 500 shapes for a best matching dual shape for a given primary shape takes 30 minutes using the fast reject filtering. Figure 9 lists some of the dihedral tiling patterns generated by our system.

Our method focuses on the shape geometry (i.e., the shape contour) as a means to preserve visual appearance. We compare our method dual tiling visual quality with [21]. We show in Figure 10 a gradual deformation (transmutation) to achieve the sky-and-water pattern of [21]. The comparison shows that our method better preserves the contour geometry and thus the shape visual appearance and quality.

We note that given two arbitrary input shapes, the results may be less meaningful due to large deformations in the simultaneous optimizations. Refer to Figure 11. Thus, we recommend the

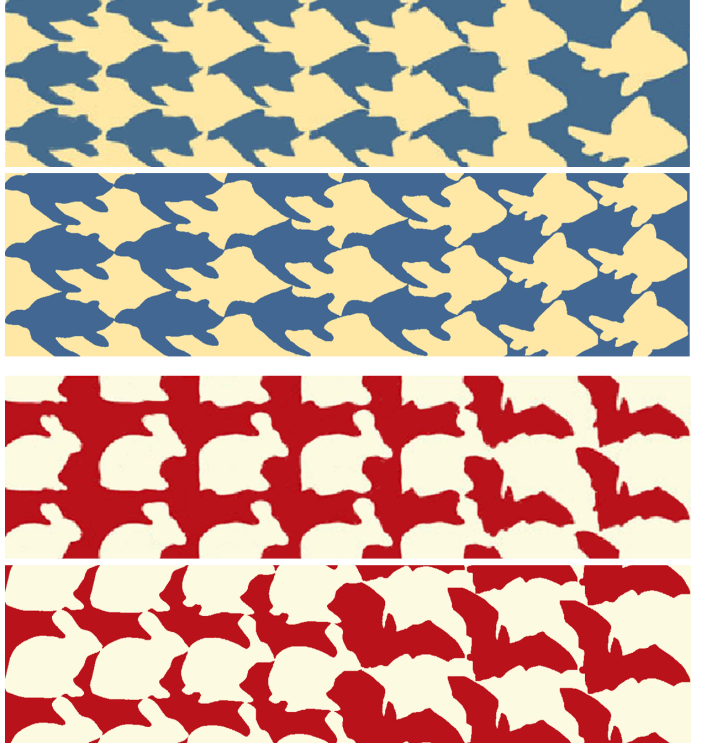


Figure 10: Comparison between the results of [21] (upper row) and our results (lower row). In our results, the turtles and rabbits are connected, respectively.

users to assign one shape as the input and trust the dataset to obtain a set of reasonable results. Of course, the input shape cannot be close to simple convex.

3D Fabrication and Applications. We apply our dihedral tiling to the generation of customized 3D shape textures that can be 3D printed. Figure 12 shows several 3D models with our dual shape textures.

Given the meaningful partitions of solid and hollow spaces, the dual patterns produce interesting light and shadow effects, which imply a great potential for designing customized lampshades. Figure 13 shows 3D models textured with our dual shape

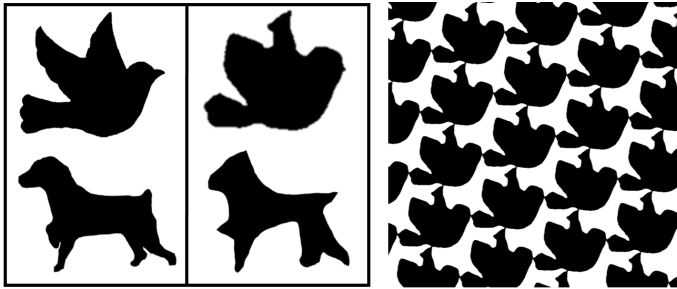


Figure 11: A failure example. Left: two input shapes, dove (as in Figure 8) and dog. Middle: the resulted patterns with too much compromission. Right: the tessellation result.

Escher tiling. They are fabricated by an SLA-based printer and projected with custom lights to demonstrate the solid and hollow dual pattern effect. **SLA or FDM based 3D printing for the decorative 3D models** may require support structures. We did remove the support materials for the four models manually, which is a bit tedious. Hence, we recommend dual-nozzle 3D printers with soluble support material, or powder based 3D printing techniques such as SLS and Binder Jetting. Table 1 summarizes the statistics for the fabricated results.

Parameters	Kitten#1	Kitten#2	Bunny	Sphere
Size (cm)	(8,12,2,7.5)	(7,6,7,10.8)	(10,8,10)	(10,10,10)
Volume (cm ³)	22.6	14.3	17.5	35
#Tiles	167	106	117	146

Table 1: Statistics of fabricated results (Figure 13 from left to right). The size is represented as (length, width, height). Row #Tiles lists the number of hollowing tiles for each model.

We can also relax the mutual surrounding constraints for each tile, such that each element has connections with two neighbors that belong to the same shape type. Thus, both patterns can be fabricated in one connected piece, as shown in Figure 14. This significantly speeds up the printing process of the dual tiles and allows for efficient utilization of the manufacturing process.

The interaction between the dual shapes and structures makes ground for novel applications. We demonstrate further applications along this path by adding joints to the connectors of some of the dual shapes. For example, given the swan-and-lily patterns, we add one rotation hinge (Figure 15) to horizontal lily tiles. This allows the lily pattern to rotate with one degree of freedom simulating the behavior of window blinds. Blocking and control of light using our 3D manufactured custom Escher blinds is demonstrated in Figure 16.

We also add ball joints to our tiles (Figure 15). A ball joint allows a limited range of smooth movement in all directions, and thus brings a larger degree of freedom for the patterns. Such joints are all support-free and can be 3D printed in one piece without postprocessing or meticulous assembly. Both models in Figures 15 and 16 are fabricated by a standard desktop FDM-based printer.

Due to their controllability and continuous tessellation of the plane, dihedral tessellations are also natural candidates for halftoning. Since the tessellation structure is fixed, we control the halftoning amount by the tile scale parameter. Thus, we dilate tiles at different scales by controlling the distance between the center of the tile and the contour line of the target shape. The resulting halftone patterns are shown in Figure 17.

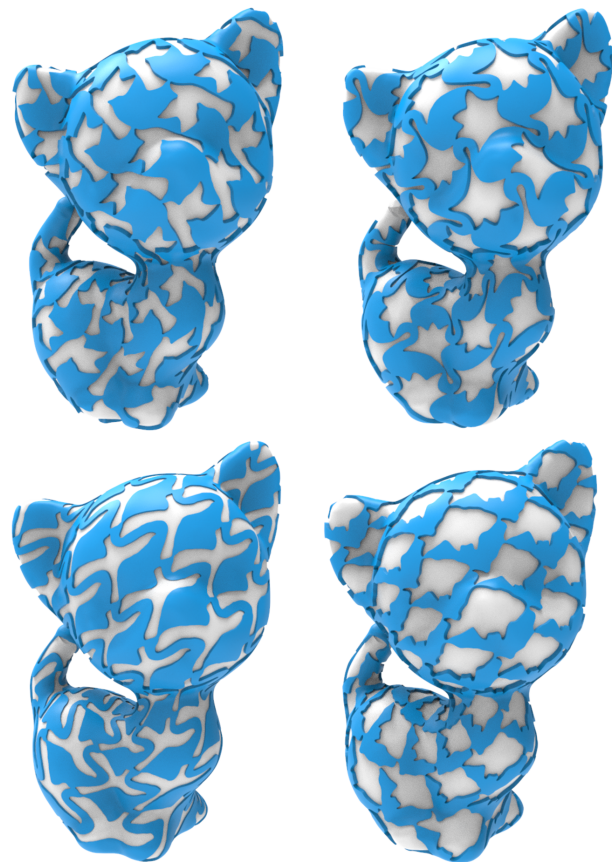


Figure 12: Applying our printable Escher dual-shape tilings onto the 3D kitten.

6. Conclusions

In this paper, we present a novel approach to model and fabricate Escher dual-shape tilings from user-defined shapes. To conform with 3D printability requirements, our tiling computation accounts for strength and connectivity. A key feature of our method is that the dual shape patterns utilize both solid and hollow spaces. Thus, one shape is mapped to solid structure and the second shape is mapped to hollow background, optimizing both spaces simultaneously. The interaction between the dual shapes makes ground for novel applications. We demonstrate the applicability of our method to 3D textures with light shading, window blinds, etc.

Limitations. The current approach has several limitations. First, our technique utilizes a 2D parametrization of the 3D shapes in the computation of 3D printable dual tiles. In the case of complex topologies, parametrization may result in significant seams that affect the visual quality of our models. **Although the seams are limited to less salient parts such as the bottom of the bunny, distortions due to the parametrization are sometimes inevitable, like the bunny's ears.** Nevertheless, the problem of parametrization is orthogonal to our focus on fabricable dual Escher tiles. **Second, the structural enhancement basically follows standard techniques. It would be more effective to integrate the structural optimization with the tile design framework.** Thirdly, the types of tiling rules are relatively limited, yielding simplistic patterns. There are certainly more complex tiling rules that can be used to generate dense tessellations. Fourthly, the quality of the results strongly depends on the input shapes. If the user inputs some complex or special shapes, it may not be able to generate appropriate dense results. The last is that the inter-



Figure 13: 3D printed models textured by our dual-shape tiling. A light source emanates through the hollow tiles in the pattern.

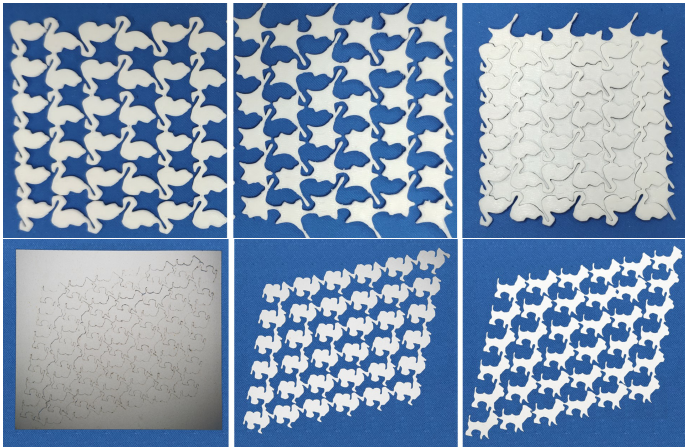


Figure 14: Upper row: The swan and lily shapes are 3D printed in one piece, separately. Both pieces can combine together with full cover of the space. Lower row: The dual shapes are jointly fabricated by digital cutting and later separated into two connected pieces (camel and dog).

action between different tiles due to joints positioning may yield collisions.

Future work. A natural future work direction is to incorporate parametrization and periodic dual tessellations in a unified optimization framework. Thus, we consider seams generations and the tiles periodic nature conjointly. This will allow positioning seams with minimal interference to the tiles periodicity. We would also integrate the strength enhancement with tiling design and consider optimizing the shape in a semantic level. Another possibility for future work is to explore more complex tiling configuration and to allow tiling with better appearance preservation. We are also excited by exploring novel applications for tiles with different joints. In general, generating exciting tiling deformations considering cloth deformations, wrinkles, and other different dynamic effects is a promising idea.

References

- [1] R. Prévost, E. Whiting, S. Lefebvre, O. Sorkine-Hornung, Make it stand: balancing shapes for 3d fabrication, ACM Transactions on Graphics 32 (4) (2013) 1. doi:10.1145/2461912.2461957.
- [2] M. Bächer, E. Whiting, B. Bickel, O. Sorkine-Hornung, Spin-it: optimizing moment of inertia for spinnable objects, ACM Transactions on Graphics 33 (4) (2014) 1–10. doi:10.1145/2601097.2601157.
- [3] W. Chen, X. Zhang, S. Xin, Y. Xia, S. Lefebvre, W. Wang, Synthesis of filigrees for digital fabrication, ACM Transactions on Graphics 35 (4) (2016) 98:1–98:13.
- [4] C. Schumacher, B. Thomaszewski, M. Gross, Stenciling: Designing structurally-sound surfaces with decorative patterns, Computer Graphics Forum 35 (5) (2016) 101–110. doi:10.1111/cgf.12967.
- [5] N. Umetani, A. Panotopoulou, R. Schmidt, E. Whiting, Printone: Interactive resonance simulation for free-form print-wind instrument design, ACM Transactions on Graphics 35 (6) (2016) 184:1–184:14.
- [6] H. Zhao, L. Lu, Y. Wei, D. Lischinski, A. Sharf, D. Cohen-Or, B. Chen, Printed perforated lampshades for continuous projective images, ACM Transactions on Graphics 35 (5) (2016) 154:1–154:11. doi:10.1145/2907049. URL <http://doi.acm.org/10.1145/2907049>
- [7] N. J. Mitra, M. Pauly, Shadow art, ACM Transactions on Graphics 28 (5) (2009) 156:1–156:7. doi:10.1145/1618452.1618502. URL <http://doi.acm.org/10.1145/1618452.1618502>
- [8] H. Peng, L. Lu, L. Liu, A. Sharf, B. Chen, Fabricating QR codes on 3d objects using self-shadows, Computer-Aided Design 114 (2019) 91–100. doi:10.1016/j.cad.2019.05.029.
- [9] M. Shugrina, A. Shamir, W. Matusik, Fab forms: customizable objects for fabrication with validity and geometry caching, ACM Transactions on Graphics 34 (4) (2015) 100:1–100:12. doi:10.1145/2766994.
- [10] D. Schattschneider, M.C. Escher: Visions of Symmetry, W.H. Freeman, 1990.
- [11] W. Chen, Y. Ma, S. Lefebvre, S. Xin, J. Martínez, W. Wang, Fabricable tile decors, ACM Transactions on Graphics 36 (6) (2017) 175:1–175:15.
- [12] A. W. Dress, The 37 combinatorial types of regular “heaven and hell” patterns in the euclidean plane, MC Escher: Art and Science (1986) 35–43.
- [13] B. Grünbaum, G. C. Shephard, Tilings and patterns, Freeman, 1987.
- [14] C. S. Kaplan, D. H. Salesin, Escherization, in: Proceedings of the 27th An-

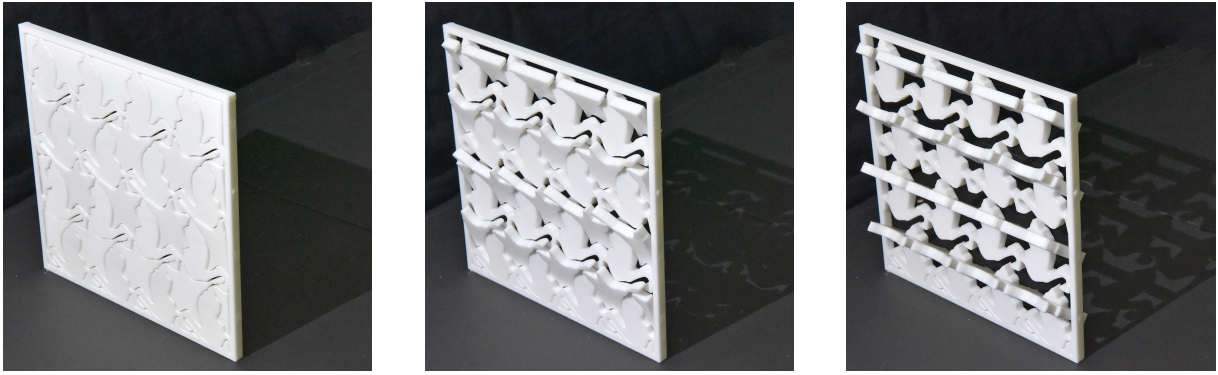


Figure 16: The decorative window blinds made by adding hinges along horizontal tiles. Left to right, controlling the amount of light passing through by rotating the lilies blinds to allow more light.

- nual Conference on Computer Graphics and Interactive Techniques, SIGGRAPH '00, ACM Press/Addison-Wesley Publishing Co., New York, NY, USA, 2000, pp. 499–510.
- [15] C. S. Kaplan, D. H. Salesin, Dihedral escherization, in: Proceedings of Graphics Interface 2004, GI '04, Canadian Human-Computer Communications Society, 2004, pp. 255–262.
- [16] J. Yen, C. Séquin, Escher sphere construction kit, in: Proceedings of the 2001 Symposium on Interactive 3D Graphics, I3D '01, ACM, New York, NY, USA, 2001, pp. 95–98.
- [17] M. Howison, C. H. Séquin, Cad tools for creating space-filling 3d escher tiles, Computer-Aided Design and Applications 6 (2009) 737–748.
- [18] K. Sugihara, Computer-aided generation of escher-like sky and water tiling patterns, Journal of Mathematics and the Arts 3 (4) (2009) 195–207. doi: 10.1080/17513470903185626.
- [19] H. Koizumi, K. Sugihara, Maximum eigenvalue problem for escherization, Graph. Comb. 27 (3) (2011) 431–439.
- [20] S. Ono, M. Kisanuki, H. Machii, K. Mizuno, Creation support for escher-like tiling patterns by interactive genetic algorithms, in: SIGGRAPH Asia 2014 Posters, SA '14, ACM, New York, NY, USA, 2014, pp. 9:1–9:1.
- [21] S. Lin, C. C. Morace, C. Lin, L. Hsu, T. Lee, Generation of escher arts with dual perception, IEEE Transactions on Visualization and Computer Graphics 24 (2) (2018) 1103–1113. doi:10.1109/TVCG.2017.2660488.
- [22] S. Zhou, C. Jiang, S. Lefebvre, Topology-constrained synthesis of vector patterns, ACM Transactions on Graphics 33 (6) (2014) 215:1–215:11. doi: 10.1145/2661229.2661238.
- [23] J. Dumas, A. Lu, S. Lefebvre, J. Wu, C. Dick, By-example synthesis of structurally sound patterns, ACM Transactions on Graphics 34 (4) (2015) 137:1–137:12. doi:10.1145/2766984.
- [24] J. Martínez, J. Dumas, S. Lefebvre, L.-Y. Wei, Structure and appearance optimization for controllable shape design, ACM Transactions on Graphics 34 (6) (2015) 229:1–229:11. doi:10.1145/2816795.2818101.
- [25] J. Zehnder, S. Coros, B. Thomaszewski, Designing structurally-sound ornamental curve networks, ACM Transactions on Graphics 35 (4) (2016) 99:1–99:10.
- [26] C. Schüller, R. Poranne, O. Sorkine-Hornung, Shape representation by zipables, ACM Transactions on Graphics 37 (4) (2018) 78:1–78:13. doi: 10.1145/3197517.3201347.
- [27] R. Silvers, Photomosaics, Henry Holt and Co., Inc., New York, NY, USA, 1997.
- [28] A. Hausner, Simulating decorative mosaics, in: Proceedings of the 28th annual conference on Computer graphics and interactive techniques - SIGGRAPH 2001, ACM Press, 2001. doi:10.1145/383259.383327.
- [29] V. Milenkovic, K. Daniels, Translational polygon containment and minimal enclosure using mathematical programming, International Transactions in Operational Research 6 (5) (1999) 525–554. doi:10.1111/j.1475-3995.1999.tb00171.x.
- [30] J. Kim, F. Pellacini, Jigsaw image mosaics, ACM Transactions on Graphics 21 (3). doi:10.1145/566654.566633.
- [31] W. Hu, Z. Chen, H. Pan, Y. Yu, E. Grinspun, W. Wang, Surface mosaic synthesis with irregular tiles, IEEE Transactions on Visualization and Computer Graphics 22 (3) (2016) 1302–1313. doi:10.1109/tvcg.2015.2498620.
- [32] K. C. Kwan, L. T. Sinn, C. Han, T.-T. Wong, C.-W. Fu, Pyramid of arclength descriptor for generating collage of shapes, ACM Transactions on Graphics 35 (6) (2016) 229:1–229:12. doi:10.1145/2980179.2980234.
- [33] W. Yang, J. Feng, 2d shape morphing via automatic feature matching and hierarchical interpolation, Computers & Graphics 33 (3) (2009) 414–423. doi:10.1016/j.cag.2009.03.007.
- [34] N. Alajlan, M. Kamel, G. Freeman, Geometry-based image retrieval in binary image databases, IEEE Transactions on Pattern Analysis and Machine Intelligence 30 (6) (2008) 1003–1013. doi:10.1109/tpami.2008.37.
- [35] L. Liu, L. Zhang, Y. Xu, C. Gotsman, S. J. Gortler, A local/global approach to mesh parameterization, Computer Graphics Forum 27 (5) (2008) 1495–1504. doi:10.1111/j.1467-8659.2008.01290.x.
- [36] M. Kazhdan, H. Hoppe, Screened poisson surface reconstruction, ACM Transactions on Graphics 32 (3) (2013) 1–13. doi:10.1145/2487228.2487237.
- [37] R. Ralph, Mpeg-7 data set, <http://www.dabi.temple.edu/shape/MPEG7/dataset.html>.



Figure 17: Dual-shape tiles Halftoning.